

# Experimental and theoretical evidence of universality in superfluid vortex reconnections

Piotr Z. Stasiak<sup>a,1</sup>, Yiming Xing<sup>b,c</sup>, Yousef Alihosseini<sup>b,c</sup>, Carlo F. Barenghi<sup>a</sup>, Andrew Baggaley<sup>a,d</sup>, Wei Guo<sup>b,c</sup>, Luca Galantucci<sup>e,a</sup>, and Giorgio Krstulovic<sup>f</sup>

This manuscript was compiled on April 3, 2025

The minimum separation between reconnecting vortices in fluids and superfluids obeys a universal scaling law with respect to time. The pre-reconnection and the post-reconnection prefactors of this scaling law are different, a property related to irreversibility and to energy transfer and dissipation mechanisms. In the present work, we determine the temperature dependence of these prefactors in superfluid helium from experiments and a numeric model which fully accounts for the coupled dynamics of the superfluid vortex lines and the thermal normal fluid component. At all temperatures, we observe a pre- and post-reconnection asymmetry similar to that observed in other superfluids and in classical viscous fluids, indicating that vortex reconnections display a universal behaviour independent of the small-scale regularising dynamics. We also numerically show that each vortex reconnection event represents a sudden injection of energy in the normal fluid. Finally we argue that in a turbulent flow, these punctuated energy injections can sustain the normal fluid in a perturbed state, provided that the density of superfluid vortices is large enough.

reconnections | superfluids | vortices | turbulence

Reconnections are the fundamental events that change the topology of the field lines in fluids and plasmas during their time evolution. Reconnections thus determine important physical properties, such as mixing and inter-scale energy transfer in fluids (1), or solar flares and tokamak instabilities in plasmas (2). The nature of reconnections is more clearly studied if the field lines are concentrated in well-separated filamentary structures: vortices in fluids and magnetic flux tubes in plasmas. In superfluid helium this concentration is extreme, providing an ideal context: superfluid vorticity is confined to vortex lines of atomic thickness (approximately  $a_0 \approx 10^{-10}$  m); a further simplification is that, unlike what happens in ordinary fluids, the circulation of a superfluid vortex is constrained to the quantized value  $\kappa = h/m = 9.97 \times 10^{-8}$  m<sup>2</sup>/s, where  $m$  is the mass of one helium atom and  $h$  is Planck's constant.

It was in this superfluid context that it was theoretically and experimentally recognized (3–9) that reconnections share a universal property irrespective of the initial condition: the minimum distance between reconnecting vortices,  $\delta^\pm$ , scales with time,  $t$ , according to the form

$$\delta^\pm(t) = A^\pm(\kappa|t - t_0|)^{1/2}, \quad [1]$$

where  $t_0$  is the reconnection time, and the dimensionless prefactors  $A^-$  and  $A^+$  refer respectively to before ( $t < t_0$ ) and after ( $t > t_0$ ) the reconnection. The same scaling law was then found for reconnections in ordinary viscous fluids (10). In the case of a pure superfluid at temperature  $T = 0$  K, theoretical work based on the Gross-Pitaevskii equation (GPE) has shown that  $A^+ > A^-$ , that is, after the reconnection, vortex lines move away from each others faster than in the initial approach; this result has been related to irreversibility (11, 12). Indeed, a geometrical constraint imposes (12) that a piece of vortex length needs to be “deleted” during the reconnection process. In the GP model, this loss is possible by the emission of a rarefaction pulse created immediately after the reconnection (6, 13) which removes some of the kinetic energy and momentum of the vortex configuration. This vortex energy loss depends on the ratio  $A^+/A^-$ , which in turn defines the approaching angle of collision between the vortices, together with other several geometrical quantities (7, 12). The temporal asymmetry  $A^+ > A^-$  can be thus interpreted as a non-trivial manifestation of irreversibility, as it originates from an ideal hydrodynamic process independent of the small-scale regularisation mechanism of the fluid.

## Significance Statement

Vortex reconnections are fundamental events that create and sustain turbulence in ordinary fluids (water, air) and in quantum fluids (superfluid helium, Bose-Einstein condensates). In this first joint experimental/theoretical study of reconnections in superfluids, we experimentally demonstrate the time-irreversible character of reconnecting quantum vortices in superfluid helium: their separation dynamics is faster than their approach dynamics. This asymmetry, and its consequent irreversible dynamics, is a universal feature of reconnections, as it has been predicted, numerically, also for other bosonic and fermionic superfluids and for ordinary fluids. Besides the topology, reconnections are also important for the energetics. We find that each reconnection injects superfluid energy into the thermal normal fluid, maintaining it in a dynamically perturbed state.

Author affiliations: <sup>a</sup>School of Mathematics, Statistics and Physics, Newcastle University, Newcastle upon Tyne, NE1 7RU, United Kingdom; <sup>b</sup>National High Magnetic Field Laboratory, 1800 East Paul Dirac Drive, Tallahassee, Florida 32310, USA; <sup>c</sup>Mechanical Engineering Department, FAMU-FSU College of Engineering, Tallahassee, Florida 32310, USA; <sup>d</sup>Department of Mathematics and Statistics, Lancaster University, Lancaster, LA1 4YF, United Kingdom; <sup>e</sup>Istituto per le Applicazioni del Calcolo “M. Picone” IAC CNR, Via dei Taurini 19, 00185 Roma, Italy; <sup>f</sup>Université Côte d'Azur, Observatoire de la Côte d'Azur, CNRS, Laboratoire Lagrange, Boulevard de l'Observatoire CS 34229 - F 06304 NICE Cedex 4, France

The authors declare no competing interest.

<sup>1</sup>To whom correspondence should be addressed. E-mail: p.stasiak@newcastle.ac.uk

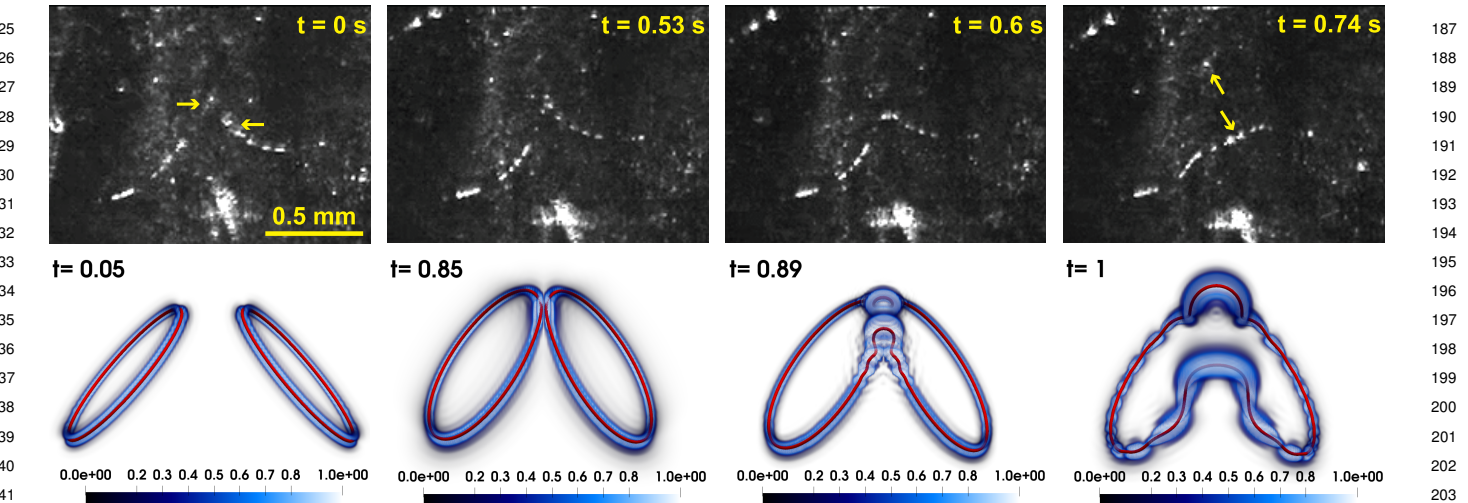


**Fig. 1.** *Top row:* Images showing tracer particles trapped on reconnecting vortices in superfluid helium at 1.65 K. The arrows denote the vortices before and after the reconnection. The first two images show that the vortices approach each other before the reconnection, which occurs at  $t = 0.58$  s. After the reconnection, the resulting vortices start to move apart, as shown in the last two images. *Bottom row:* Oblique collision of two circular vortex rings at different (dimensionless) times, here in units of  $\tau = 0.183$ s. The superfluid vortex lines are represented by red tubes (the radius has been greatly exaggerated for visual purposes); the scaled normal fluid enstrophy  $\omega^2/\omega_{max}^2$  is represented by the blue volume rendering.

Indeed, in classical fluid vortex reconnections, although the definition of  $A^+$  is more delicate as circulation is not necessarily conserved, the same asymmetry  $A^+ > A^-$  was reported (10). Instead of the generation of rarefaction pulses, like in the case of  $T = 0$  superfluids, close to the reconnection, the classical fluid creates a series of thin secondary structures that can be then efficiently dissipated by viscous dissipation. We note that the reconnection event also generates wavepackets of Kelvin waves about either side of the reconnection cusp, which propagate outward (visible in the bottom panel of Fig 1). These waves are the fundamental mechanism transferring superfluid kinetic energy to smaller scales (14, 15). The interaction of Kelvin waves with the normal fluid has recently been studied (16, 17).

The case of superfluid helium at non-zero temperatures is more intriguing. Most experiments are performed at  $T > 1$  K, a regime in which in addition to quantum vortices, thermal excitations constitute a viscous liquid called the *normal fluid*. The normal fluid can steal energy from filaments and dissipate it by viscous effects, opening in that way more routes towards irreversibility. Modern visualisation techniques rely on hydrogen/deuterium tracer particles to decorate superfluid vortices (4, 18–20). Numerous studies have provided insight into the post-reconnection dynamics and the prefactor  $A^+$ , but much less is known about  $A^-$  from experiments due to the challenges of visualising vortices approaching a reconnection.

The aim of this Letter is to investigate the role played by the normal fluid in the reconnection dynamics. In particular, given the temperature dependence of the normal fluid's properties, we study experimentally and numerically the temperature dependence of the prefactors  $A^+$  and  $A^-$  and numerically investigate the energy injected in the normal fluid. To achieve this aim we need a more powerful model than the GPE to account not only for the dynamics of the superfluid vortices, but also for the dynamics of the normal fluid. We show that at non-zero temperatures Eq. (1) and the relation  $A^+ > A^-$  hold true, in agreement with experiments, revealing,

for the first time, a temperature dependence of  $A^+/A^-$ . In addition, we show that a vortex reconnection represents an unusual kind of punctuated energy injection into the normal fluid which acts alongside the well-known (continual) friction. When applied to superfluid turbulence, this last result implies that, if the vortex line density (hence the frequency of reconnections) is large enough, vortex reconnections can maintain the normal fluid in a perturbed state.

## Results

**Scaling law.** In the experiment, two reconnections were observed where both  $A^+$  and  $A^-$  could be identified and calculated, at  $T = 1.65$ K and  $T = 2$ K, plotted as orange triangles in Fig. 2b. We also analysed six additional experimental observations of the *post-reconnection* dynamics only (vertical dot-dashed lines). All were consistent with the  $\delta^{1/2}$  scaling with  $A^+$  in the range 1.2–4.2, plotted as vertical lines in Fig. 2b. Their corresponding minimal distances are displayed in the inset of Fig 2a. The pre-reconnection factor  $A^-$  lies within the 0.4–0.6 range, consistent with the results of the numerics, and a clear temperature effect between a superfluid component majority and normal fluid component majority. In the case of the Hopf link we have performed 147 simulations (49 across 3 temperatures) as shown in Fig. 2a and verified Eq. (1) for the minimum distance  $\delta^\pm$ . The prefactors  $A^\pm$  have been computed in the shaded region of the figure. In the pre-reconnection regime ( $t < t_0$ ) we observe a clear segregation of the values of  $A^-$  due to temperature: the minimum distance grows more rapidly with time if the temperature is lowered. In stark contrast, there is almost no memory of the temperature in the post-reconnection regime ( $t > t_0$ ).

At  $T = 0$  K, our calculations for superfluid helium (black symbols in Fig. 2b) are in good agreement with previous results obtained with the GPE (11) (green diamonds), showing irreversible dynamics. In addition, the computed

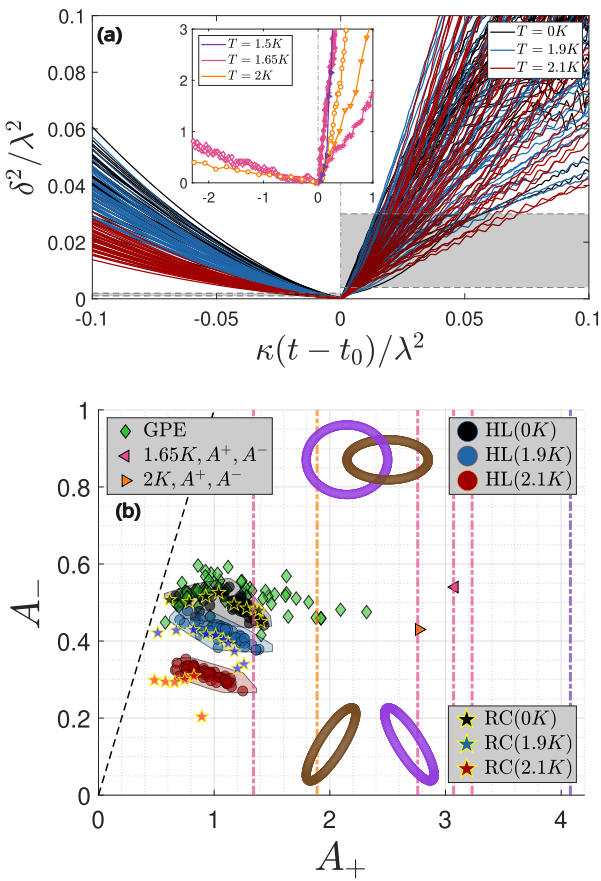


**Fig. 2.** (a): Time evolution of the (dimensionless) minimum distance squared  $\delta^2$  plotted versus (dimensionless)  $\kappa(t - t_0)$  for the Hopf link reconnections at  $T = 0K$ ,  $1.9K$  and  $2.1K$  (black, blue and red respectively). The grey shaded areas are the regions used to estimate the prefactors  $A^\pm$ . Inset: Experimental superfluid helium data. (b): Comparison of all prefactors: Hopf links (HL, circles), ring collisions (RC, stars with yellow outline), GPE-data from Villois *et. al.* (11) (green diamonds) and experimental results from this study (triangles and vertical dot-dashed lines). The shaded areas associated with each colour represent the convex hull of errors for each temperature and the black dashed line represents the theoretical bound for  $A^+/A^-$ . Schematic rendering of initial conditions are included.

values of  $A^- \approx 0.4$ - $0.6$  at  $T = 0$  K are consistent with analytical calculations (21, 22). At non-zero temperatures, our results confirm the irreversibility of vortex reconnections observed at  $T = 0$  as  $A^+$  is always larger than  $A^-$ . Importantly, this asymmetry is recovered in all our simulations, regardless of their initial condition. The same asymmetry between  $A^+$  and  $A^-$  at non-zero temperatures has been observed for reconnections in finite-temperature Bose-Einstein condensates (23), although in this work the system is not homogeneous (the condensate is confined by a harmonic trap) and the thermal component is a ballistic gas, not a viscous fluid. Note that the vortex reconnections in classical viscous fluids reported in (10) also display a clear 1/2 power-law scaling for the minimum distance with  $A^- \approx 0.3$ - $0.4$ , which again shows good agreement with our results. The scaling law (Eq. 1) and the range of values of  $A^-$  hence appear to have a universal character in vortex reconnections, independently of the nature of the fluid, classical or quantum.

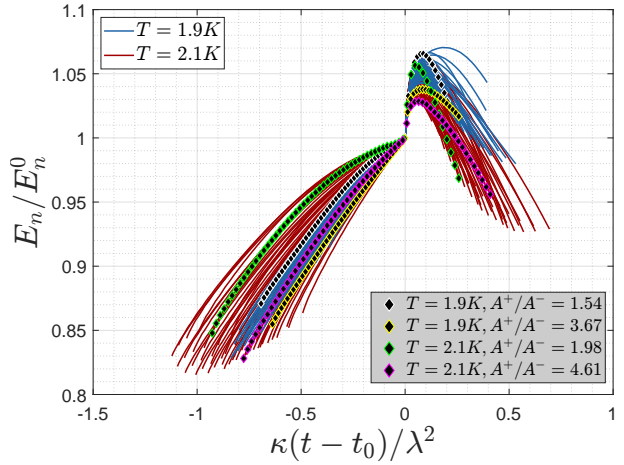


**Fig. 3.** Normal fluid kinetic energy  $E_n$  scaled by  $E_n^0$  (the kinetic energy at  $t = t_0$ ), plotted versus (dimensionless)  $\kappa(t - t_0)$  for the Hopf link reconnections. Black diamonds represent the simulations with minimum and maximum prefactor ratios  $A^+/A^-$  at  $T = 1.9$  K and  $T = 2.1$  K respectively.

**Energy Injection.** The normal fluid impacts the dynamics of reconnecting superfluid vortices via the temperature dependent mutual friction coefficients. Conversely, the motion of superfluid vortices involved in the reconnection process influence, significantly, the dynamics of the normal fluid. Figure 3 indeed shows that the normal fluid energy,  $E_n$ , suddenly increases at the reconnection time by an amount ( $\approx 5\%$ ) which is smaller but comparable to the continuous energy increase as vortex lines approach each other. Indeed the curvature  $\zeta = |\mathbf{s}''|$  of the vortex line spikes at  $t = t_0$  when the reconnection cusp is created, and, in the first approximation (24), the magnitude of the energy injected in the normal fluid per unit time  $I$  is proportional to the strength of the mutual friction force  $\mathbf{F}_{ns}$  which scales as  $|\mathbf{F}_{ns}(\mathbf{s})| \propto |\dot{\mathbf{s}} - \mathbf{v}_n| \propto |\dot{\mathbf{s}}| \propto \zeta$ . This sudden transfer of energy (16) from the superfluid vortex configuration to the normal fluid is the origin of the small scale normal fluid enstrophy structures which are visible in Fig. 1.

The total energy injected into the normal fluid by the reconnection,  $\Delta E_n$ , which hereafter we refer to as the energy jump, is defined as

$$\Delta E_n = \max [E_n(t > t_0)] - E_n^0, \quad [2]$$

where  $E_n^0 = E_n(t_0)$  is the normal fluid kinetic energy at  $t = t_0$ . Normalized energy jumps are plotted in Fig. 4 as a function of the ratio  $A^+/A^-$ . Here, we observe that the larger  $A^+/A^-$  is, the smaller the normal fluid excitation is.

The emission of the sound pulse at the vortex reconnection (13) which is typical of the GPE model is absent in our incompressible hydrodynamic approach. To model this effect, the change of vortex length,  $\Delta L$ , created by the vortex reconnection algorithm is always negative by construction (25), because, in the local induction approximation to the Biot-Savart law, the superfluid incompressible kinetic energy,  $E_s$ , is proportional to the vortex length,  $L$ . Such procedure ensures that at  $T = 0$  K when a reconnection occurs  $\Delta E_s \propto \Delta L < 0$ . Consequentially, in the absence of any dissipative normal fluid, the superfluid energy  $E_s$  that would be transferred to the sound pulse, normalized with its value  $E_s^0$  at reconnection, is  $-\Delta L/L_0$ . If these normalized energy

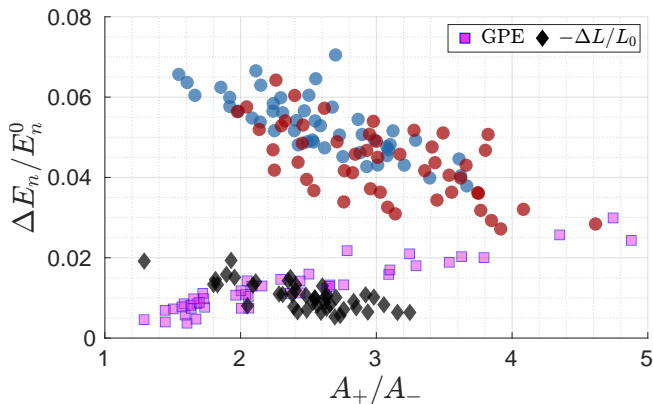


**Fig. 4.** Normalized energy jumps  $\Delta E_n/E_n^0$  for Hopf link reconnections. The solid black diamonds are the normalized change in line length  $\Delta L/L_0$  in the  $T = 0$  K case. Blue and red circles correspond to  $T = 1.9$  K and  $T = 2.1$  K respectively. The purple squares are from GPE simulations of Villois et al. (11).

jumps (black diamonds in Fig. 4) are compared to the results obtained with the compressible GPE (11) (purple squares) we find a good agreement, confirming that the model we employ, is suitable for the investigation of the features of single reconnection events.

**Implications for turbulence.** Our numerical results have implications for our understanding of quantum turbulence (26). A fully developed turbulent tangle of vortices is characterized by its vortex line density  $\mathcal{L}$  (vortex length per unit volume); the frequency of vortex reconnections per unit volume is  $f = (\kappa/6\pi)\mathcal{L}^{5/2} \ln(\mathcal{L}^{-1/2}/a_0)$  (27). From Fig. 3 we estimate the normal fluid reconnection relaxation time  $\tau_n$  as the time after reconnection at which the normal fluid energy  $E_n/E_0$  has decayed to the pre-reconnection level: in our dimensionless units,  $\kappa\tau_n \approx 0.25$ . Using this timescale, we estimate that the average vortex line density that is corequired to sustain the normal fluid in a perturbed state via frequent vortex reconnections is approximately  $\mathcal{L} \approx 10^7$  to  $10^8 \text{ m}^{-2}$ . Experiments in  ${}^4\text{He}$  (28–32) and in  ${}^3\text{He}$  (33) can achieve vortex line densities much larger than this.

Above the vortex line density threshold, the increase of normal fluid energy generated by the reconnection will not have time to decay before the subsequent reconnection occurs, which will add again more energy. In this manner, the normal fluid energy will not decay to zero, but will increase in time. In general, such finite amplitude normal fluid disturbances constantly injected by reconnections may become relevant for various superfluid helium systems. One example is the oscillatory flows, which are widely studied in superfluid helium using vibrating wires and forks. At low frequency, perturbations which start at finite-amplitude rather than infinitesimal-amplitude level have enough time to become of order one (hence visible and destabilizing) in the supercritical part of the cycle (34). A second example is pipe flow, again relevant to helium experiments, which is known to suffer from finite-amplitude instabilities (35). This effect clearly needs further investigations.

## Discussion

We have conducted an experiment using passive particle tracers and a suite of numerical simulations of vortex

reconnections over a wide range of temperatures using a model of  ${}^4\text{He}$  which accounts for the coupled dynamics of superfluid and normal fluid components. We have verified the scaling law of the minimum vortex distance  $\delta^\pm = A^\pm(\kappa|t-t_0|)^{1/2}$  and found that the approach prefactor  $A^-$  has a clear temperature dependence independent of the geometry in both experiments and numerics, in contrast to the separation prefactor  $A^+$ . The prefactors are in good agreement with GPE simulations (11, 23) and classical fluid reconnections (10) revealing that vortex reconnections display a universal behaviour, linked to irreversible vortex energy dissipation, regardless of the nature of the fluid (classical or quantum) and of temperature, *i.e.* regardless of the small scale energy transfer mechanism. It is worth noting that the behaviour, as a function of  $A^+/A^-$ , of the energy injected in the normal fluid (at  $T > 0$ ) and of the energy transferred to sound (at  $T = 0$ ) (11, 13) is dissimilar: the former decreases as  $A^+/A^-$  increases, the latter the opposite. This likely arises from the distinct physics governing the loss of superfluid incompressible kinetic energy: mutual friction at  $T > 0$ , quantum pressure at  $T = 0$ . We have also found that a reconnection event suddenly injects an amount of energy into the normal fluid which is comparable to the energy transferred by friction during the vortex approach. Applying these results to turbulence, we have compared the decay time of the normal fluid structures created by a reconnection to the frequency of reconnections in a vortex tangle, and argued that, if the vortex line density is large enough, these punctuated energy injections should sustain the normal fluid in a perturbed state, which may lead to a new type of turbulence.

## Materials and Methods

**Experimental Method.** To visualize the reconnection dynamics, we decorate the vortices using solidified deuterium ( $D_2$ ) tracer particles of density  $202.8 \text{ kg/m}^3$  (36)) and mean radius  $1.1 \times 10^{-6} \text{ m}$  (37, 38). These particles are generated by injecting a  $D_2/{}^4\text{He}$  gas mixture into the superfluid helium bath (37, 39) as described in the Supplementary Material (SM). When the particles are near the vortices, they become trapped inside their cores because of the Bernoulli pressure arising from the circulating superfluid flow. A thin laser sheet is used to illuminate the particles, and their motion is recorded at 200 Hz by a camera positioned at a right angle to the laser sheet. A high-quality reconnection event, observed at  $T = 1.65$  K and capturing both the pre- and post-reconnection dynamics, is shown in Fig. 1 as an example. Note that according to GP simulations (40) the transfer of energy and momentum between particle and vortex does not modify the approaching rates significantly. Reconnection events reported in this work have been captured in multiple experiments, either following particle injection or long time (*i.e.*, 30–60 s) after towing a grid through superfluid helium. (this is also supported by the scaling symmetry of the system which allows us to draw conclusion for length-scales relevant to experiments).

**Numerical Method.** We follow the approach of Schwarz (41) which exploits the vast separation of length scales between the vortex core  $a_0$  and any other relevant distance, in particular the average distance between vortices,  $\ell$ , in the case of turbulence. Vortex lines are described as space curves  $\mathbf{s}(\xi, t)$  where  $\xi$  is arclength. The equation of motion of the vortex lines is

$$\dot{\mathbf{s}}(\xi, t) = \mathbf{v}_s + \frac{\beta}{(1+\beta)} [\mathbf{v}_{ns} \cdot \mathbf{s}'] \mathbf{s}' + \beta \mathbf{s}' \times \mathbf{v}_{ns} + \beta' \mathbf{s}' \times [\mathbf{s}' \times \mathbf{v}_{ns}], \quad [3]$$

where  $\dot{\mathbf{s}} = \partial \mathbf{s} / \partial t$ ,  $\mathbf{s}' = \partial \mathbf{s} / \partial \xi$  is the unit tangent vector,  $\mathbf{v}_n$  and  $\mathbf{v}_s$  are the normal fluid and superfluid velocities at  $\mathbf{s}$ ,  $\mathbf{v}_{ns} = \mathbf{v}_n - \mathbf{v}_s$ , and  $\beta, \beta'$  are temperature and Reynolds number dependent mutual

497 friction coefficients (42). The normal fluid velocity  $\mathbf{v}_n$  is described  
 498 as a classical fluid obeying the incompressible ( $\nabla \cdot \mathbf{v}_n = 0$ ) Navier-  
 499 Stokes equations:

$$500 \quad \frac{\partial \mathbf{v}_n}{\partial t} + (\mathbf{v}_n \cdot \nabla) \mathbf{v}_n = -\frac{1}{\rho} \nabla p + \nu_n \nabla^2 \mathbf{v}_n + \frac{\mathbf{F}_{ns}}{\rho_n}, \quad [4]$$

502 where  $\mathbf{F}_{ns}$  is the mutual friction force that couples the normal  
 503 fluid and the superfluid vortices, and acts as an internal injection  
 504 mechanism. In Eq. Eq. (4),  $\rho = \rho_n + \rho_s$ , where  $\rho_n$  and  $\rho_s$  are  
 505 the normal fluid and superfluid densities,  $p$  is the pressure, and  
 506  $\nu_n$  is the kinematic viscosity of the normal fluid. Equations (3)  
 507 and (4) are solved in dimensionless form by rescaling them by  
 508 the characteristic time  $\tau$  and length  $\lambda$ . The algorithm for vortex  
 509 reconnections is standard (25). We consider two distinct initial  
 510 vortex configurations at three temperatures  $T = 0$  K, 1.9 K and  
 511 2.1 K corresponding to the superfluid fractions  $\rho_s/\rho = 100\%$ , 58%  
 512 and 26%. To compare with experiments, the unit of length is  
 513 set to  $\lambda = 1.59 \times 10^{-4}$  m, and the time units to  $\tau = 0.183$  s at  
 514  $T = 0$  K and 1.9 K, and  $\tau = 0.242$  s at  $T = 2.1$  K, see also the SM  
 515 for details. All configurations lead to a vortex reconnection. The  
 516 first configuration consists of two vortex rings of (dimensionless)  
 517 radius  $R \approx 1$  in a tent-like shape which collide obliquely making  
 518 an initial angle  $\alpha$  with the vertical direction, as shown in Fig. 1,  
 519  
 520

- 521 1. J Yao, F Hussain, Vortex reconnection and turbulence cascade. *Ann. Rev. Fluid Mech.* **54**,  
 522 317 (2022).
2. IT Chapman, et al., Magnetic reconnection triggering magnetohydrodynamic instabilities  
 523 during a sawtooth crash in a tokamak plasma. *Phys. Rev. Lett.* **105**, 255002 (2010).
3. S Nazarenko, R West, Analytical solution for nonlinear Schrödinger vortex reconnection. *J.  
 524 Low Temp. Phys.* **132**, 1 (2003).
4. GP Bewley, MS Paoletti, KR Sreenivasan, DP Lathrop, Characterization of reconnecting  
 526 vortices in superfluid helium. *Proc. Nat. Acad. Sci. USA* **105**, 13707 (2008).
5. MS Paoletti, ME Fisher, DP Lathrop, Reconnection dynamics for quantized vortices. *Phys.  
 527 D* **239**, 1367–1377 (2010).
6. S Zuccher, M Calari, AW Baggaley, CF Barenghi, Quantum vortex reconnections. *Phys.  
 529 Fluids* **24**, 125108 (2012).
7. A Vilhois, D Proment, G Krstulovic, Universal and nonuniversal aspects of vortex  
 531 reconnections in superfluids. *Phys. Rev. Fluids* **2**, 044701 (2017).
8. L Galantucci, AW Baggaley, NG Parker, CF Barenghi, Crossover from interaction to driven  
 532 regimes in quantum vortex reconnections. *Proc. Nat. Acad. Sci. USA* **116**, 12204 (2019).
9. M Tylutki, G Wlazłowski, Universal aspects of vortex reconnections across the bcs-bec  
 533 crossover. *Phys. Rev. A* **103**, L051302 (2021).
10. J Yao, F Hussain, Separation scaling for viscous vortex reconnection. *J. Fluid Mech.* **900**,  
 535 R4 (2020).
11. A Vilhois, D Proment, G Krstulovic, Irreversible dynamics of vortex reconnections in quantum  
 536 fluids. *Phys. Rev. Lett.* **125**, 164501 (2020).
12. D Proment, G Krstulovic, Matching theory to characterize sound emission during vortex  
 538 reconnection in quantum fluids. *Phys. Rev. Fluids* **5**, 104701 (2020).
13. M Leadbeater, T Winiecki, DC Samuels, CF Barenghi, CS Adams, Sound emission due to  
 540 superfluid vortex reconnections. *Phys. Rev. Lett.* **86**, 1410–1413 (2001).
14. W Vinen, Decay of superfluid turbulence at a very low temperature: The radiation of sound  
 541 from a kelvin wave on a quantized vortex. *Phys. Rev. B* **64**, 134520 (2001).
15. W Vinen, J Niemela, Quantum turbulence. *J. low temperature physics* **128**, 167–231 (2002).
16. PZ Stasiak, AW Baggaley, G Krstulovic, CF Barenghi, L Galantucci, Cross-component  
 543 energy transfer in superfluid helium-4. *J. Low Temp. Phys.* (2024).
17. PZ Stasiak, et al., Inverse energy transfer in three-dimensional quantum vortex flows. *arXiv  
 544 preprint arXiv:2503.04450* (2025).
18. MS Paoletti, ME Fisher, KR Sreenivasan, DP Lathrop, Velocity statistics distinguish  
 546 quantum turbulence from classical turbulence. *Phys. review letters* **101**, 154501 (2008).
19. W Guo, M La Mantia, DP Lathrop, SW Van Sciver, Visualization of two-fluid flows of  
 548 superfluid helium-4. *Proc. Natl. Acad. Sci.* **111**, 4653–4658 (2014).
20. C Peretti, J Vessaire, Émeric Durozoy, M Gibert, Direct visualization of the quantum vortex  
 549 lattice structure, oscillations, and destabilization in rotating  $^{4}\text{He}$ . *Sci. Adv.* **9**, eadhb2899 (2023).
21. L Boué, D Khomenko, V Lvov, I Procaccia, Analytic solution of the approach of quantum  
 551 vortices towards reconnection. *Phys. Rev. Lett.* **111**, 145302 (2013).

552 and, schematically, in Fig. 2b. By changing the parameter  $\alpha$ , we  
 553 create a sample of 12 realizations at each temperature (again, see  
 554 the SM for details). The second configuration is the Hopf link,  
 555 shown schematically in Fig. 2b. It consists of two perpendicular  
 556 linked rings of radius  $R \approx 1$  with an offset in the  $xy$ -plane. By  
 557 changing the offset, we create a sample of 49 reconnections at each  
 558 temperature, as described in the SM. In all cases, normal fluid  
 559 structures generated by moving superfluid vortex rings (43), are  
 560 initially prepared to eliminate any potential transients.

**ACKNOWLEDGMENTS.** Y.M.X., Y.A., and W.G. acknowledge  
 569 the support from the Gordon and Betty Moore Foundation  
 570 through Grant DOI 10.37807/gbmf11567 and the US Department  
 571 of Energy under Grant DE-SC0020113. The experimental work  
 572 was conducted at the National High Magnetic Field Laboratory  
 573 at Florida State University, which is supported by the National  
 574 Science Foundation Cooperative Agreement No. DMR-2128556  
 575 and the state of Florida. G.K. acknowledges financial support  
 576 from the Agence Nationale de la Recherche through the project  
 577 QuantumVIW ANR-23-CE30-0024-02. P.Z.S. acknowledges the  
 578 financial support of the UCA “visiting doctoral student program”  
 579 on complex systems. Computations were carried out at the  
 580 Mésocentre SIGAMM hosted at the Observatoire de la Côte  
 581 d’Azur.

22. R S, Self-similar vortex reconnection. *C. R. Méc* **347**, 365 (2019).
23. AJ Allen, et al., Vortex reconnections in atomic condensates at finite temperature. *Phys.  
 584 Rev. A* **90**, 013601 (2014).
24. L Galantucci, G Krstulovic, C Barenghi, Friction-enhanced lifetime of bundled quantum  
 585 vortices. *Phys. Rev. Fluids* **8**, 014702 (2023).
25. AW Baggaley, The sensitivity of the vortex filament method to different reconnection models.  
*J. Low Temp. Phys.* **168**, 18 (2012).
26. CF Barenghi, L Skrbek, KR Sreenivasan, *Quantum Turbulence*. (Cambridge University  
 588 Press), (2023).
27. CF Barenghi, DC Samuels, Scaling laws of vortex reconnections. *J. Low Temp. Phys.* **136**,  
 589 281 (2004).
28. KW Schwarz, CW Smith, Pulsed-ion study of ultrasonically generated turbulence in  
 591 superfluid  $^4\text{He}$ . *Phys. Lett. A* **82**, 251–254 (1981).
29. FP Milliken, KW Schwarz, CW Smith, Free Decay of Superfluid Turbulence. *Phys. Rev. Lett.*  
 593 **48**, 1204–1207 (1982).
30. PE Roche, CF Barenghi, Vortex spectrum in superfluid turbulence: Interpretation of a recent  
 594 experiment. *EPL* **81**, 36002 (2008).
31. PE Roche, et al., Vortex density spectrum of quantum turbulence. *EPL* **77**, 66002 (2007).
32. S Babuin, E Varga, L Skrbek, E Lévéque, PE Roche, Effective viscosity in quantum  
 596 turbulence: a steady state approach. *Eur. Lett.* **106**, 24006 (2014).
33. DI Bradley, et al., Decay of pure quantum turbulence in superfluid  $^3\text{He-B}$ . *Phys. Rev. Lett.*  
 598 **96**, 035301 (2006).
34. C Barenghi, C Jones, Modulated taylor–couette flow. *J. Fluid Mech.* **208**, 127–160 (1989).
35. J Peixinho, T Mullin, Finite-amplitude thresholds for transition in pipe flow. *J. Fluid Mech.*  
 600 **582**, 169–178 (2007).
36. T Xu, SW Van Sciver, Density effect of solidified hydrogen isotope particles on particle  
 602 image velocimetry measurements of  $^4\text{He}$  II flow. *AIP Conf. Proc.* **985**, 191–198 (2008).
37. Y Tang, et al., Imaging quantized vortex rings in superfluid helium to evaluate quantum  
 603 dissipation. *Nat. Commun.* **14**, 2941 (2023).
38. Y Tang, S Bao, W Guo, Superdiffusion of quantized vortices uncovering scaling laws in  
 604 quantum turbulence. *Proc. Natl. Acad. Sci. U.S.A.* **118**, e2021957118 (2021).
39. E Fonda, KR Sreenivasan, DP Lathrop, Sub-micron solid air tracers for quantum vortices  
 606 and liquid helium flows. *Rev. Sci. Instrum.* **87**, 025106 (2016).
40. U Giurato, G Krstulovic, Quantum vortex reconnections mediated by trapped particles.  
*Phys. Rev. B* **102**, 094508 (2020).
41. KW Schwarz, Three-dimensional vortex dynamics in superfluid  $^4\text{He}$ . *Phys. Rev. B* **38**, 2398  
 609 (1988).
42. L Galantucci, AW Baggaley, CF Barenghi, G Krstulovic, A new self-consistent approach of  
 610 quantum turbulence in superfluid helium. *Eur. Phys. J. Plus* **135**, 547 (2020).
43. D Kivotides, CF Barenghi, DC Samuels, Triple vortex ring structure in superfluid helium ii.  
*Science* **290**, 777 (2000).